

The Primary Interaction Vertex

Hans Wenzel

*Lawrence Berkeley National Laboratory*¹

Abstract

We present some studies about the properties of the beam during Run 1. We show position, slope, variation of the transverse profile in z and other parameters of interest. The variation of the transverse profile is also used to extract accelerator parameters like emittance, β^* and z_0 for a few Runs². For some Runs we also show how position and σ varied in time during a Run.

1 Introduction

The average position of the beam was calculated offline once per Run using tracks reconstructed in the SVX [1] [2]. In the following we describe some of the beam properties.

The interaction probability as a function of z was approximately a gaussian function with a sigma of 30 cm (see upper plot in Figure 4). The beam is a straight line and can have some offset with respect to the z axis of the tracking detectors and is also not necessarily parallel to this axis.

In a variety of physics analyses the position of the beam is used as an estimate for the primary interaction vertex and the σ of the transverse profile gives the uncertainty of this estimate. For example in the lifetime analysis the error is an important component of an unbinned likelihood fit used to extract the lifetime from the $c\tau$ -distributions therefore it is important to know the shape of the transverse profile, how it changes with z and if the position of the beam is stable in time.

¹Now: Institut für Experimentelle Kernphysik Universität Karlsruhe

²Most of these Runs were missing in the SVXBPO database and had to be processed anyhow.

In Run II CDF will be equipped with the SVT, a trigger which selects events with displaced vertices. Variations of the profile in z and any beam instabilities in time will have some impact on efficiency and signal to background ratio of the SVT.

2 Position and Slope of the Beam

Figures 1 and 2 show the position and slope of the beam during the course of Run 1. The values have been extracted from the SVXBPO ³ database. During Run 1a the beam was drifting from Run to Run. In the final months of Run 1b the beam stayed fairly stable after the misaligned quad magnets had been fixed and high luminosity was achieved. The beam slope is typically $6 \mu\text{m}/\text{cm}$ ($600 \mu\text{rad}$) in x and $-3 \mu\text{m}/\text{cm}$ ($-300 \mu\text{rad}$) in y .

3 Transverse Profile of the Beam

Figure 3 shows the profile of the beam for a given Run. Plotted is the variation of reconstructed primary vertices in the transverse plane with respect to the calculated average beam position. To ensure that the spread of the beam and not the resolution of the vertex fit is actually the dominant contribution to the width of the observed distribution we required that at least three 3d tracks with 4 hits in the SVX separated in φ were used in the vertex fit. Still the distributions shown represent the convolution of vertex resolution and the actual width of the beam we just assume that the beam dominates. In general the width here have to be regarded as an overestimate of the real width. The upper 2 plots show the two-dimensional distribution of the beam spot for a given Run during the 94-95 Running period. The lower two plots show the x and y projection respectively with a fit to a gaussian distribution superimposed. We observe that the beam is gaussian and circular. The fit of a gaussian function to the x and y projections gives a σ of $23 \mu\text{m}$ in x and $22 \mu\text{m}$ in y for this particular run. Note the Plots are averaged over the z -range covered by the two SVX modules and over the Run. One expects the σ of the beam to vary in z where $\sigma(z)$ can be expressed by the following equation [3]:

$$\sigma(z) = \sqrt{\epsilon\beta^* \times (1 + ((z - z_0)/\beta^*)^2)} \quad (1)$$

where ϵ is the transverse emittance, β^* the amplitude function at the interaction point and z_0 the z position of the minimum. Figure 5 shows the x -projection of the beam for different slices in z . The two lower plots in Figure 4 show the variation of the beam width with z for the x and y projection for a given Run. Table 1 summarizes the results of fitting function 1 to z -slices of the x and y projection of the beamprofile.

³Note the SVXBPO database besides position and slope of the beam also contains entries for the width which should be ignored!

The β^* results agree well with the values given by fermilab beams division (0.35 m) [4]. The calculated σ of the beam at $z = z_0$ (minimum) and $z - z_0 = 0.25$ m respectively are listed in Table 2 for the x and y projection. The Parameters used are the ones of Table 1. We observe that the width of the beam can vary by up to ≈ 30 % over the length of 25 cm.

Run	$emittance_x$ [$10^{-9}\pi$ rad-m]	β_x^* [m]	z_0 [m]	$emittance_y$ [$10^{-9}\pi$ rad-m]	β_y^* [m]	z_0 [m]
62984	1.69 ± 0.16	0.34 ± 0.04	0.07 ± 0.01	1.51 ± 0.09	0.30 ± 0.02	0.01 ± 0.01
63033	1.25 ± 0.05	0.38 ± 0.02	0.06 ± 0.01	0.98 ± 0.04	0.42 ± 0.02	0.01 ± 0.01
63129	1.19 ± 0.09	0.37 ± 0.03	0.05 ± 0.01	1.07 ± 0.06	0.35 ± 0.02	0.02 ± 0.01
63130	1.25 ± 0.08	0.32 ± 0.03	0.05 ± 0.01	1.01 ± 0.07	0.38 ± 0.03	0.01 ± 0.01
63149	1.14 ± 0.07	0.39 ± 0.03	0.06 ± 0.01	1.04 ± 0.05	0.36 ± 0.02	0.02 ± 0.01
63153	1.39 ± 0.09	0.34 ± 0.03	0.05 ± 0.01	1.09 ± 0.09	0.40 ± 0.04	0.01 ± 0.01
64060	1.12 ± 0.01	0.35 ± 0.04	0.04 ± 0.01	1.00 ± 0.08	0.36 ± 0.04	0.02 ± 0.01
64146	1.28 ± 0.05	0.37 ± 0.02	0.08 ± 0.01	1.12 ± 0.04	0.38 ± 0.02	0.00 ± 0.01
66556	1.28 ± 0.08	0.35 ± 0.03	0.02 ± 0.01	0.90 ± 0.1	0.45 ± 0.05	0.03 ± 0.01
68739	1.32 ± 0.04	0.36 ± 0.01	0.03 ± 0.004	1.13 ± 0.04	0.38 ± 0.01	0.00 ± 0.004
68958	1.43 ± 0.08	0.33 ± 0.02	0.01 ± 0.01	1.07 ± 0.07	0.38 ± 0.03	-0.01 ± 0.01
69005	1.10 ± 0.07	0.40 ± 0.03	0.06 ± 0.01	1.06 ± 0.06	0.39 ± 0.03	0.00 ± 0.01
69354	0.94 ± 0.06	0.41 ± 0.03	0.03 ± 0.01	0.74 ± 0.07	0.49 ± 0.05	-0.01 ± 0.01
69392	1.03 ± 0.07	0.39 ± 0.03	0.04 ± 0.01	0.99 ± 0.07	0.40 ± 0.03	0.00 ± 0.01

Table 1: *Result of fit to the width of the beam as a function of z for the x and y projection.*

4 Stability of the beam

From studies using prompt J/Ψ , $Y(1s)$ and QCD events we already know that the beam is in general very stable in time [5]. The beamposition stored in the SVXBPO database serves as a good estimate of the primary interaction vertex and shifting of the beam position contributes only an insignificant amount the error of the primary vertex.

The upper two plots in Figures 6-17 show the deviation in μm from the average beamposition as a function of time (event number) for the x and y projection respectively. For this set of Runs we observe that the position of the beam is very stable moving only a few microns over time. The exception here is Run 66556 where a drift of more than 15 microns is observed. Overall these drifts only contribute very little to the uncertainty of the primary vertex estimate and make it unnecessary to introduce

Run	$\sigma_x (z = z_0)$ [μm]	$\sigma_x z - z_0 = 0.25$ [μm]	$\sigma_y (z = z_0)$ [μm]	$\sigma_y z - z_0 = 0.25$ [μm]
62984	24	30	21	28
63033	22	26	20	24
63129	21	25	19	24
63130	20	25	20	23
63149	21	25	19	24
63153	22	27	21	25
64060	20	24	19	23
64146	22	26	21	25
66556	21	26	20	23
68739	22	27	21	25
68958	22	27	20	24
69005	21	25	20	24
69354	20	23	19	21
69392	20	24	20	23

Table 2: *The calculated σ of the beam at $z = z_0$ (minimum) and $z - z_0 = 0.25$ m respectively for the x and y projection. We observe that the width of the beam can vary by up to ≈ 30 % over the length of 25 cm.*

time depend database entries. The lower two plots show the width of the beam in μm as a function of time. Only vertices with $|z - z_0| < 10.\text{cm}$ have been used to estimate the width. A straight line fit is superimposed which gives the width as a function of event number. In general it looks like the beam gets a little bit wider over the course of a run which is what one would expect.

References

- [1] Hans Wenzel: *Fitting the beam position with the SVX* ; CDF internal note 1924 (1993)
- [2] H. Wenzel, D. Benjamin, A. Sill, D. Stuart, R. Snider: *Beamlines* ; CDF internal note 3334 (1995)
- [3] Paul Derwent *private communication*
- [4] see e.g. web pages of the Fermilab Beams Division or Phys. Rev.D, Review of Particle Properties, **54**, (1996)
- [5] Lifetime PRD in preparation

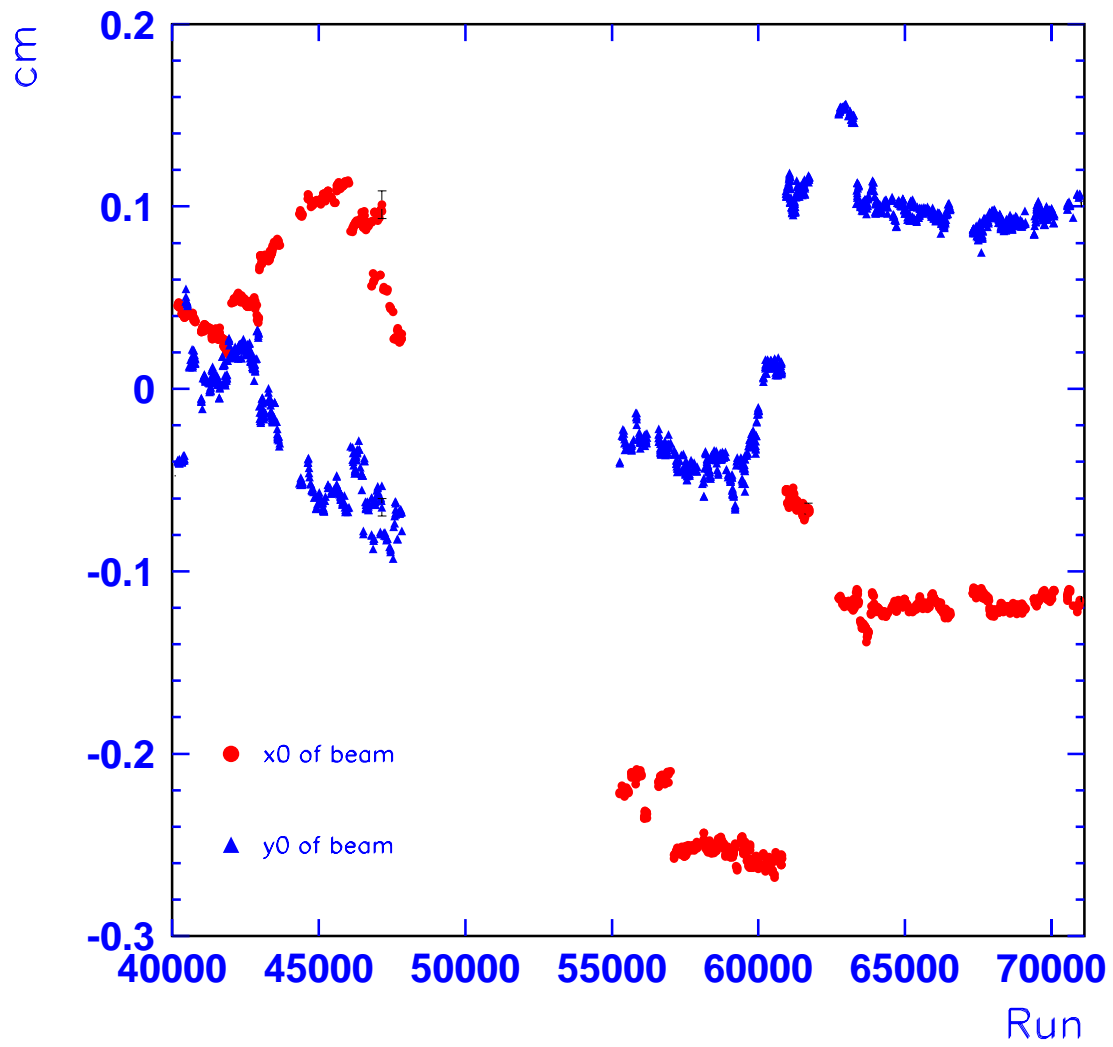


Figure 1: x_0 and y_0 of the beam as a function of Run number.

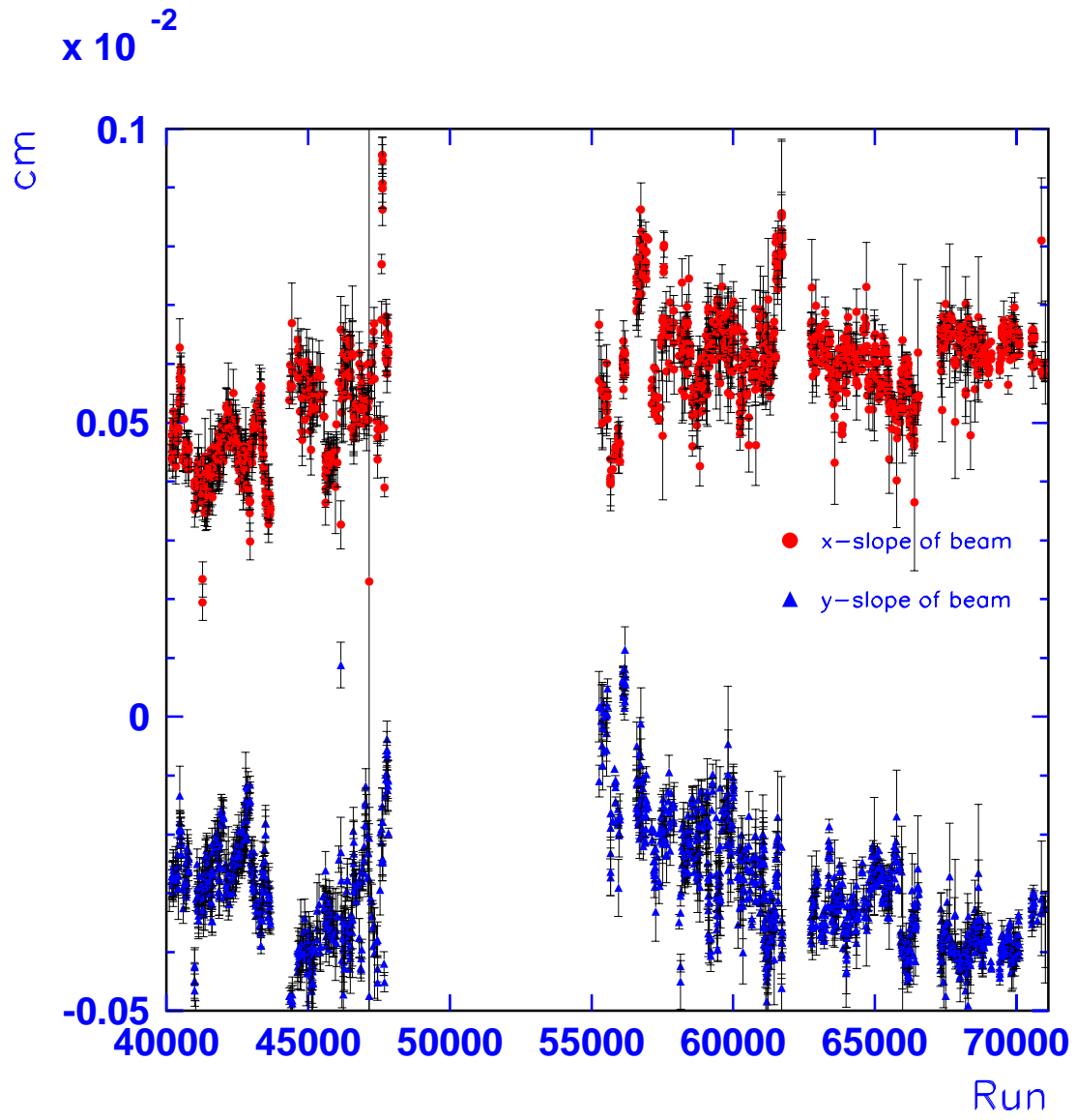


Figure 2: *Slope of the beam in x and y as a function of Run number.*

Run: 63033

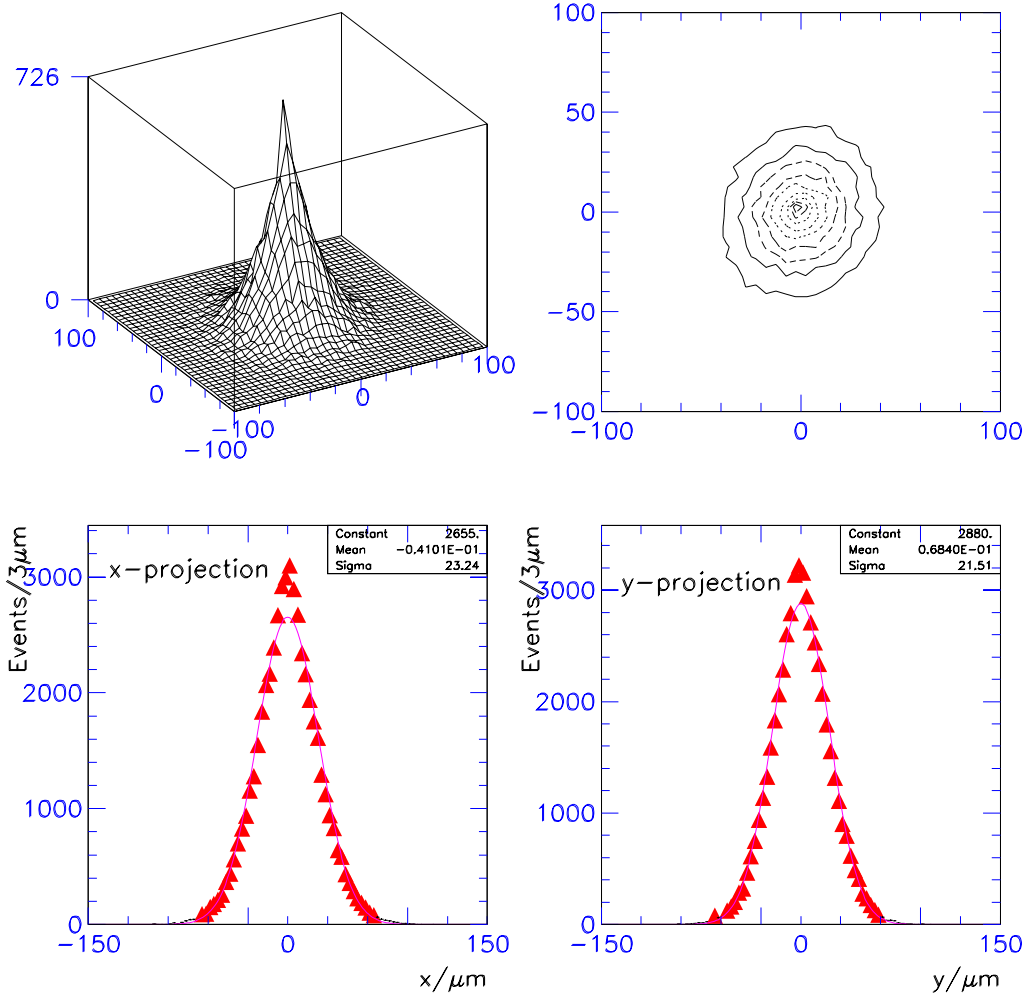


Figure 3: The upper 2 plots show the twodimensional distribution of the beam spot for a given Run during the 94-95 Running period averaged over the z -range covered by the SVX detector. The lower two plots show the x and y projection respectively. We observe that the beam is circular with an average σ of $23\ \mu\text{m}$ in x and $22\ \mu\text{m}$ in y .

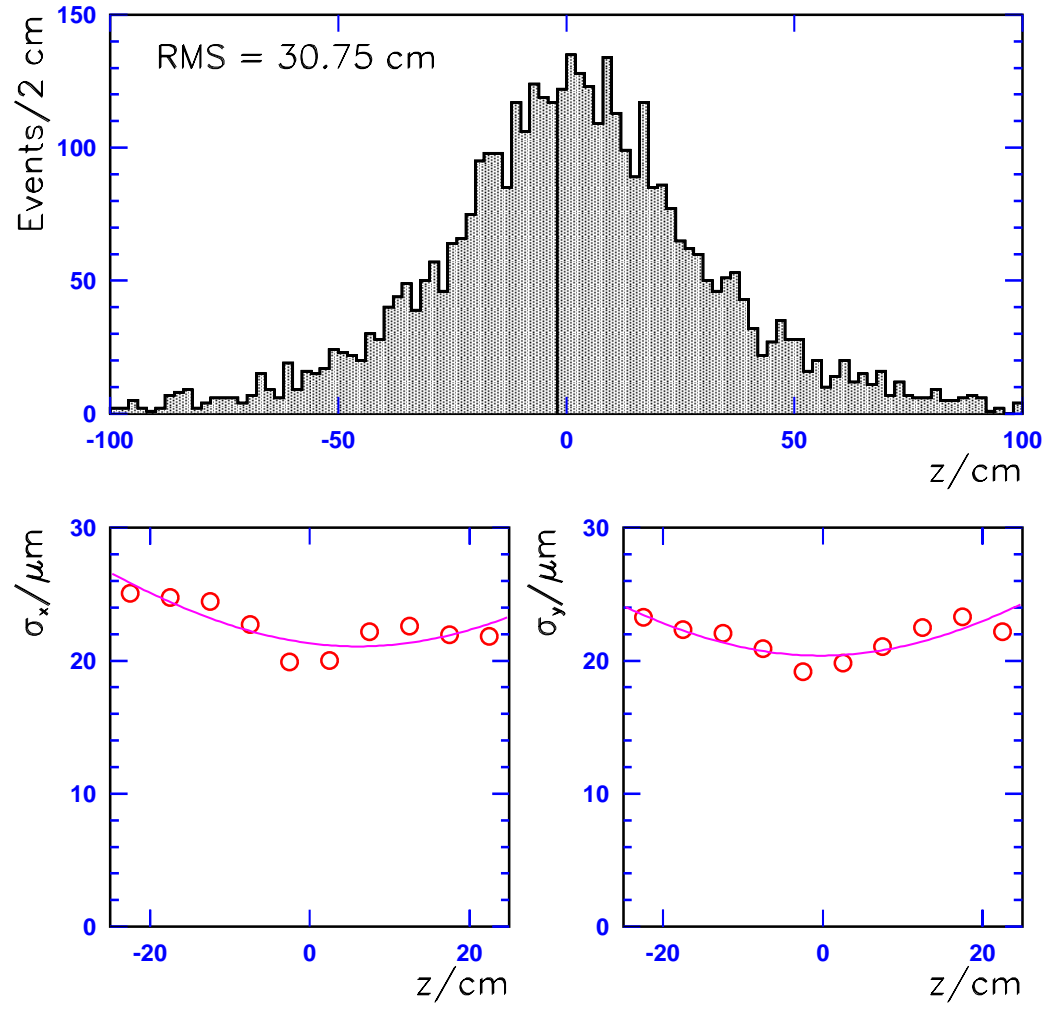


Figure 4: The upper plot shows the distribution of primary vertices in z for a typical Run. The lower two plots show the σ of the beam in x and y as a function of z with the fitted functions superimposed.

Run: 63033

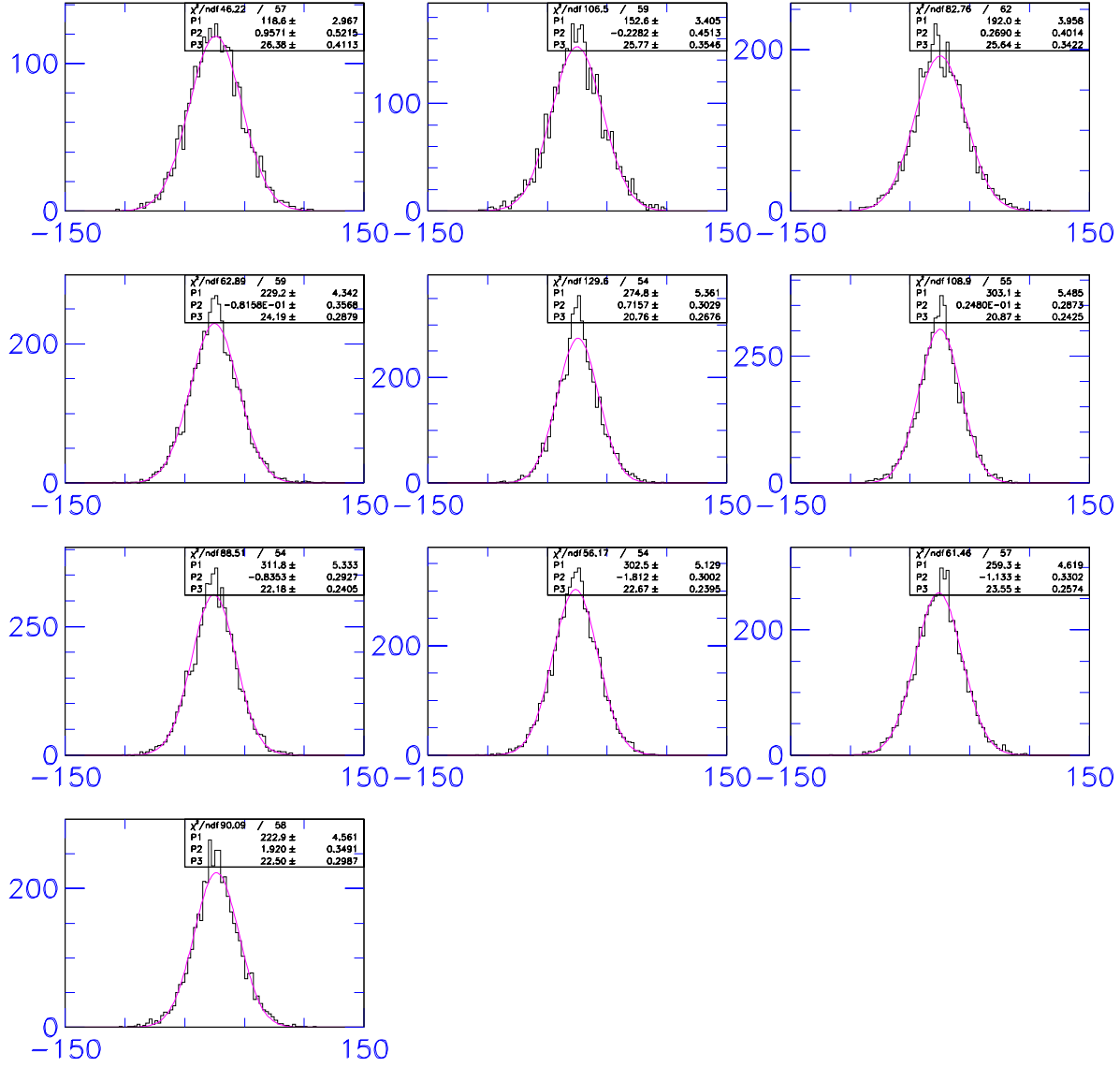


Figure 5: *x*-projection of beam profile for different slices in *z* (10 bins from -25 to +25 cm) averaged over the entire run with fitted gaussian function superimposed.

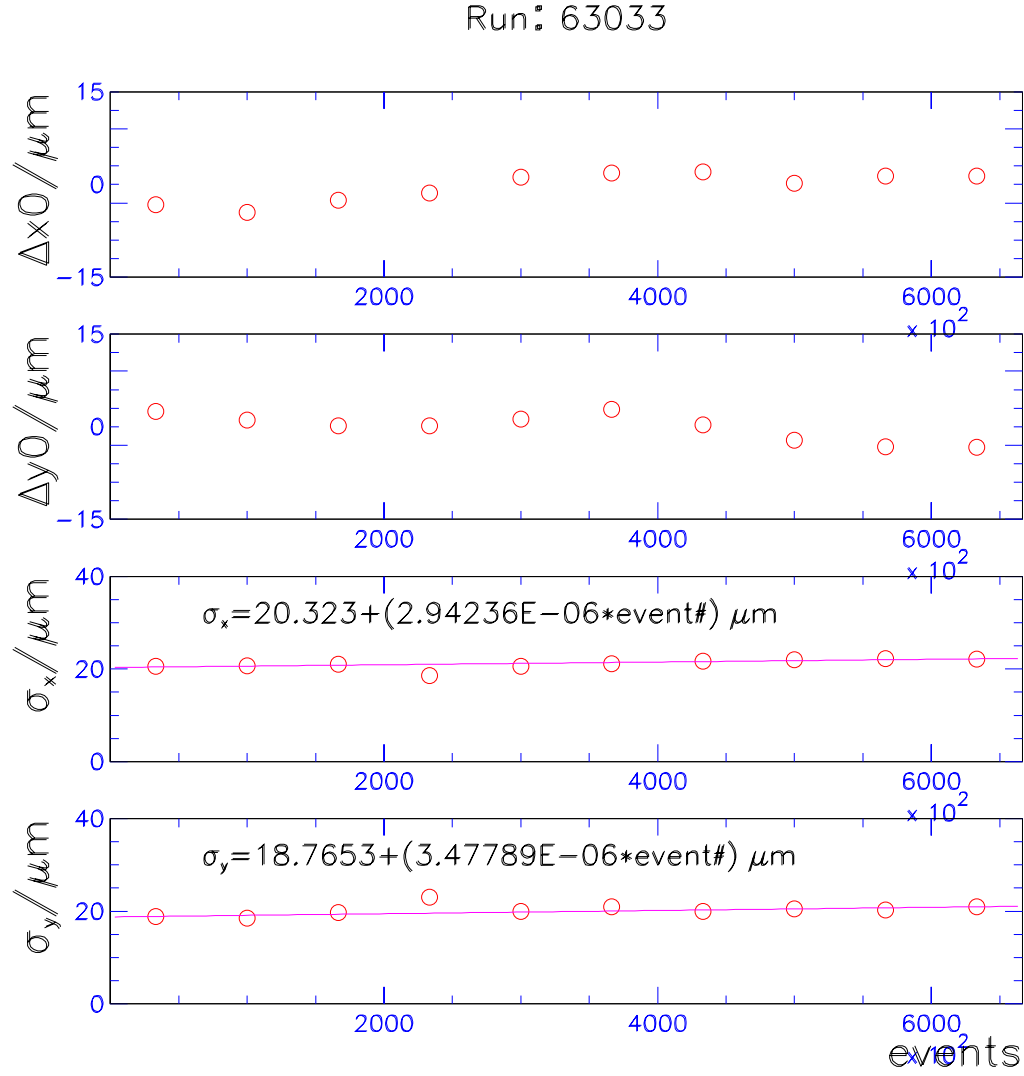


Figure 6: The upper two plots show the deviation in μm from the average beam position as a function of time (event number) for the x and y projection respectively. The lower two plots show the width of the beam in μm as a function of time. Only vertices with $|z - z_0| < 10.\text{cm}$ have been used to estimate the width.

Run: 63129

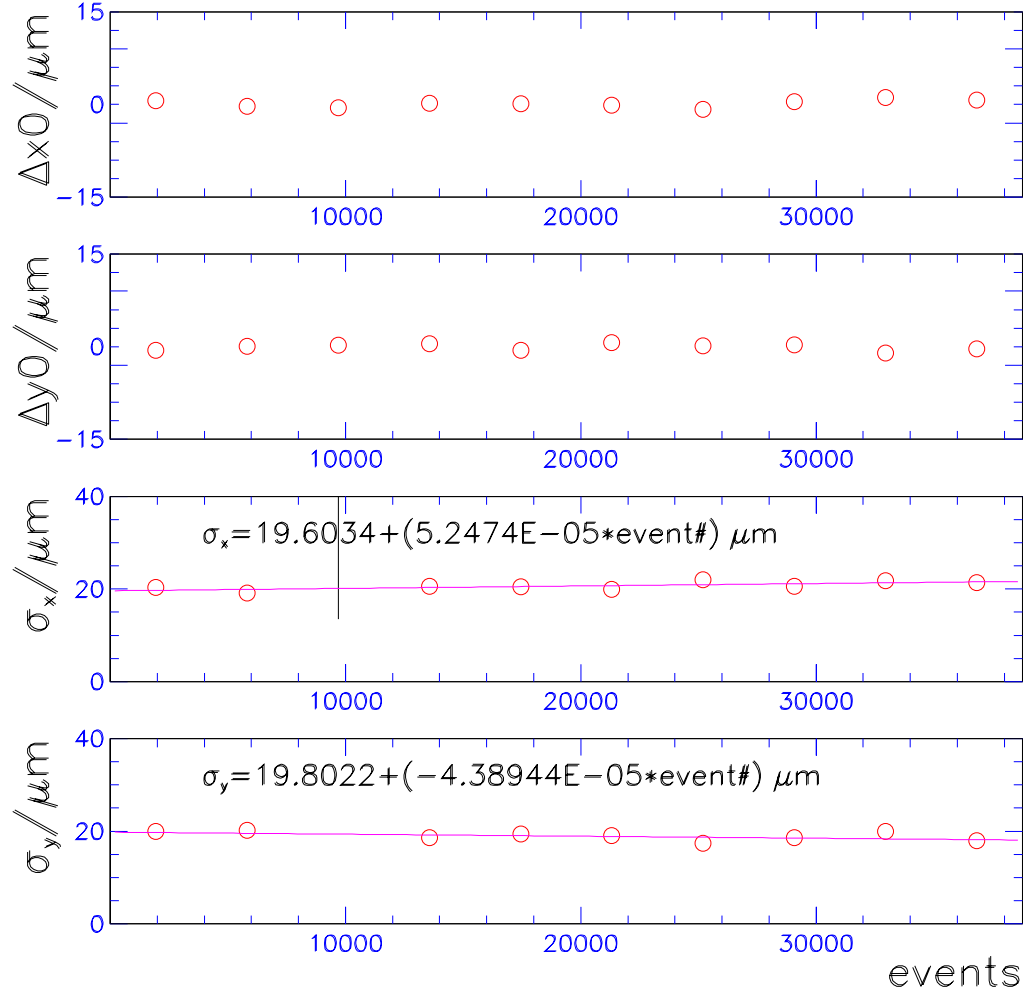


Figure 7: The upper two plots show the deviation in μm from the average beamposition as a function of time (event number) for the x and y projection respectively. The lower two plots show the width of the beam in μm as a function of time. Only vertices with $|z - z_0| < 10.\text{cm}$ have been used to estimate the width.

Run: 63130

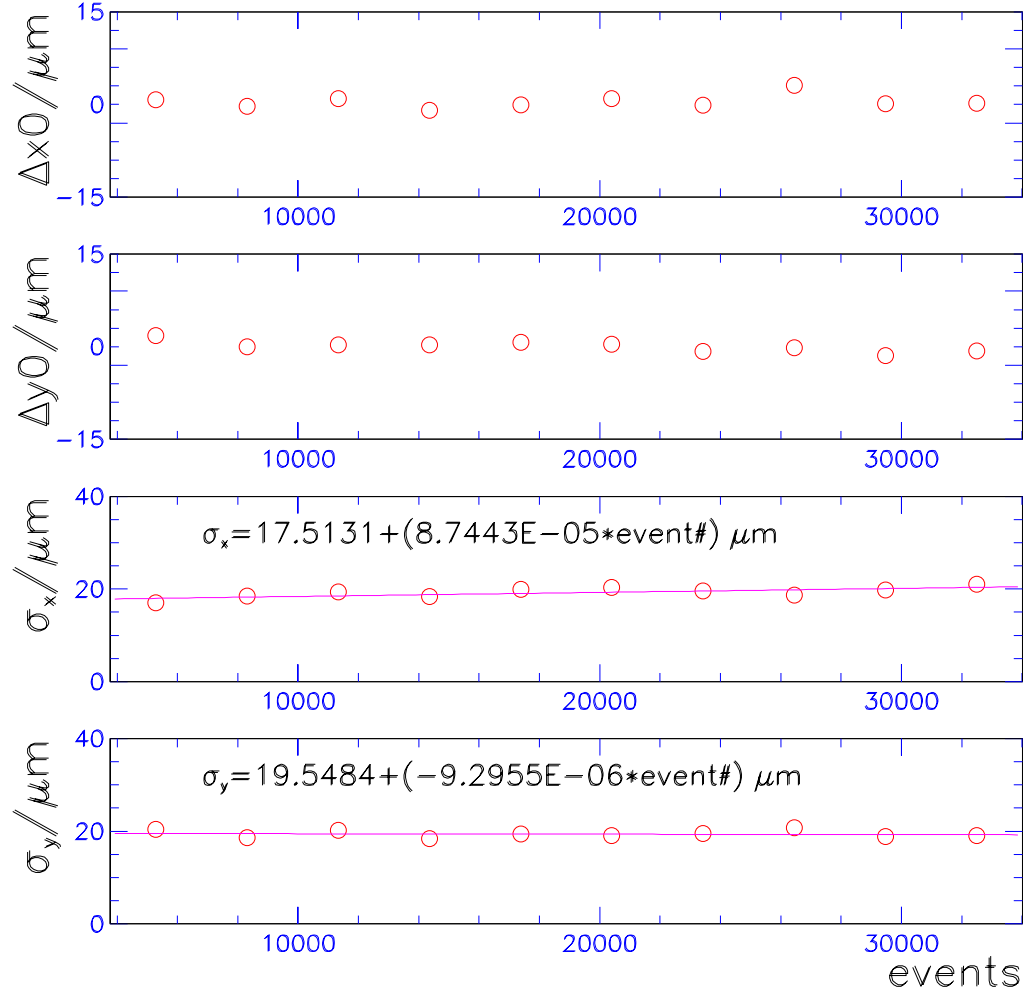


Figure 8: The upper two plots show the deviation in μm from the average beamposition as a function of time (event number) for the x and y projection respectively. The lower two plots show the width of the beam in μm as a function of time. Only vertices with $|z - z_0| < 10.\text{cm}$ have been used to estimate the width.

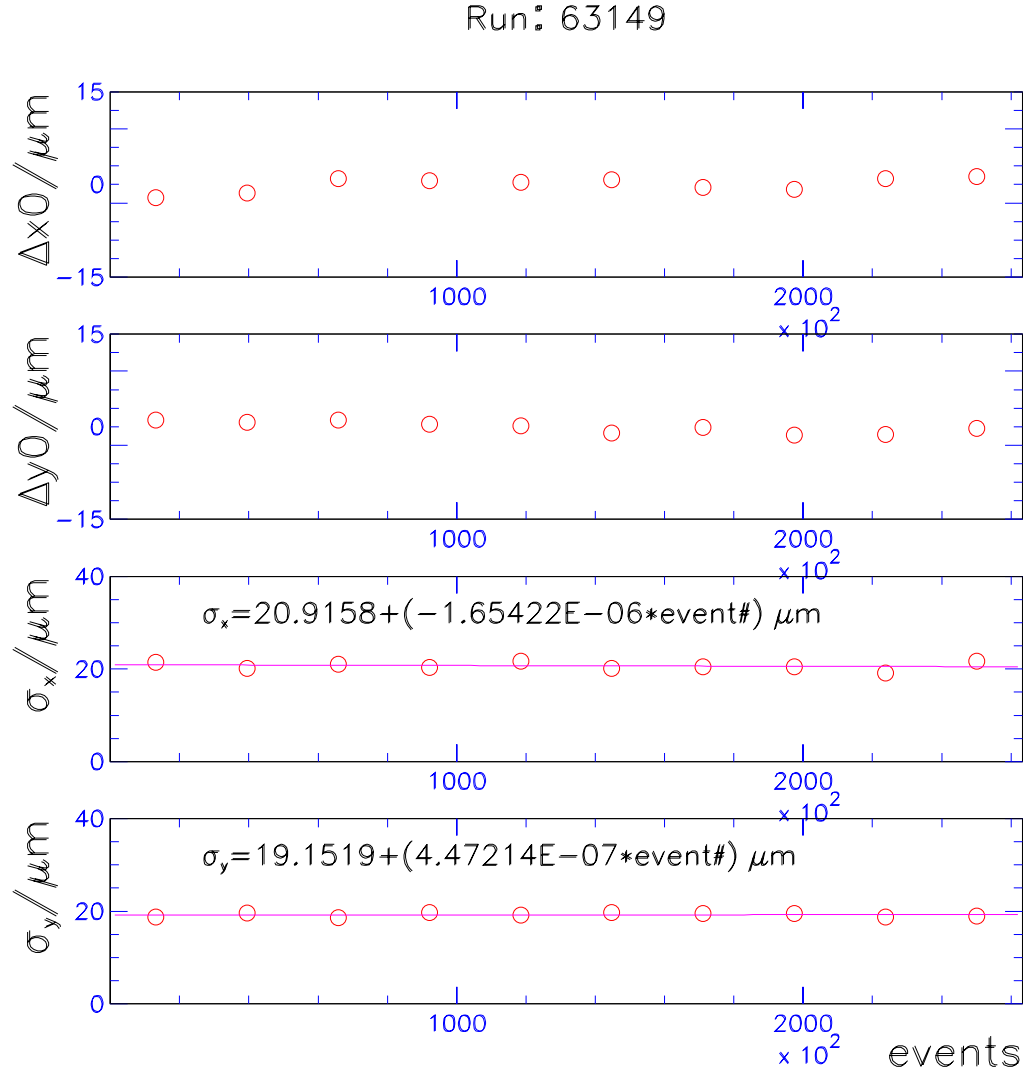


Figure 9: The upper two plots show the deviation in μm from the average beamposition as a function of time (event number) for the x and y projection respectively. The lower two plots show the width of the beam in μm as a function of time. Only vertices with $|z - z_0| < 10.\text{cm}$ have been used to estimate the width.

Run: 63153

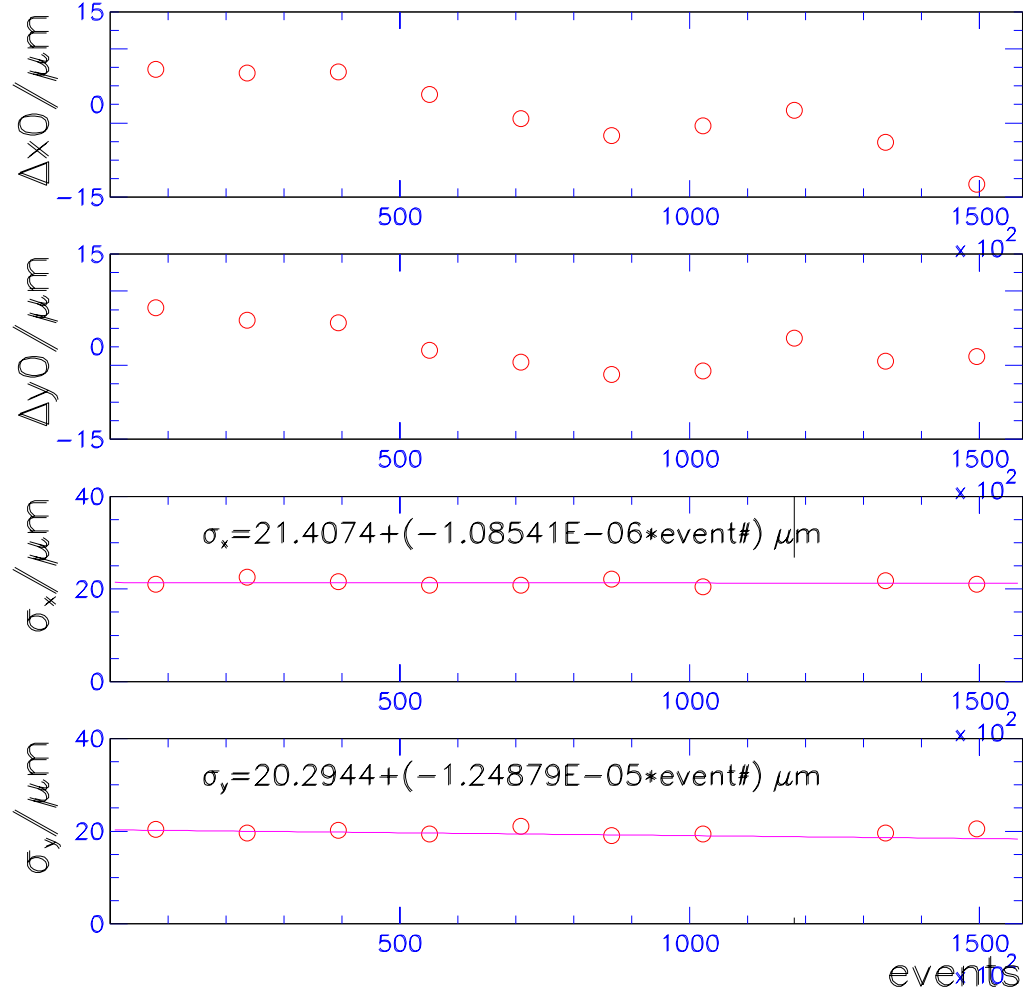


Figure 10: The upper two plots show the deviation in μm from the average beamposition as a function of time (event number) for the x and y projection respectively. The lower two plots show the width of the beam in μm as a function of time. Only vertices with $|z - z_0| < 10.\text{cm}$ have been used to estimate the width.

Run: 64060

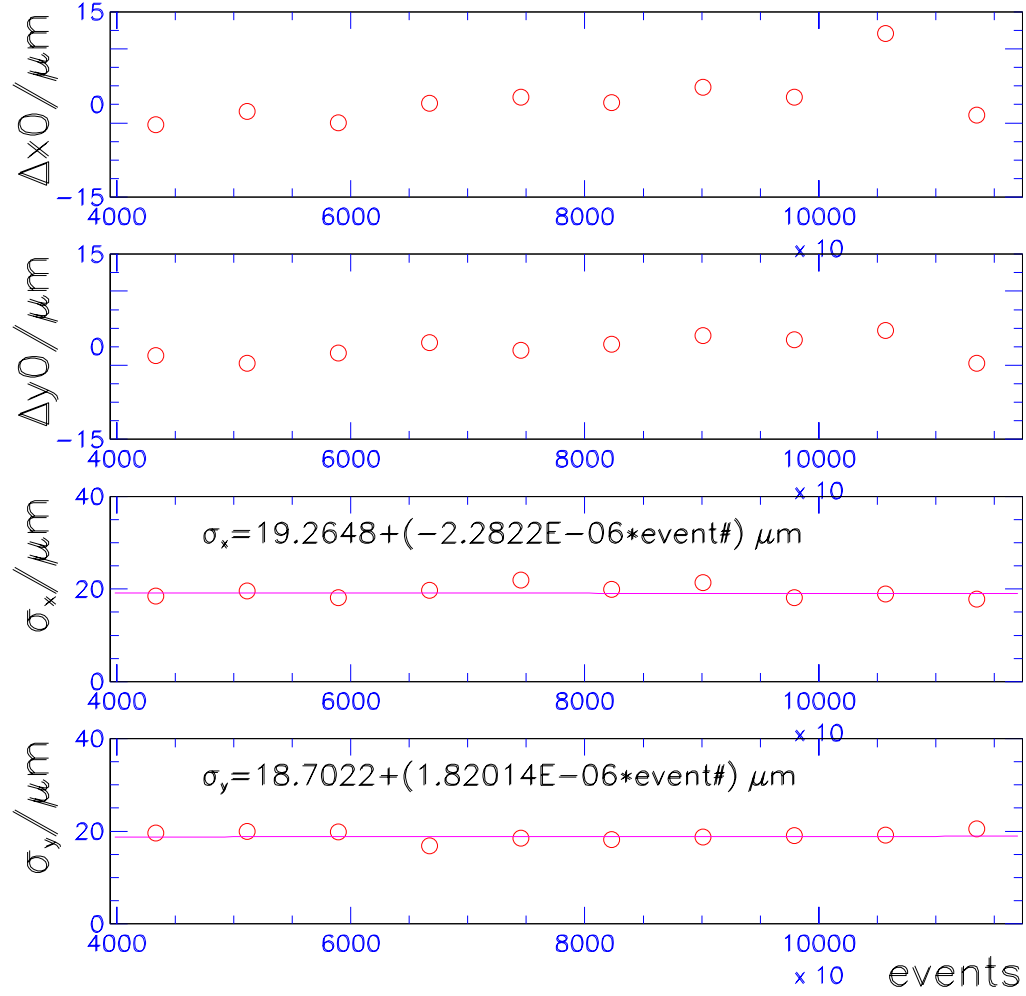


Figure 11: *The upper two plots show the deviation in μm from the average beamposition as a function of time (event number) for the x and y projection respectively. The lower two plots show the width of the beam in μm as a function of time. Only vertices with $|z - z_0| < 10.\text{cm}$ have been used to estimate the width.*

Run: 64146

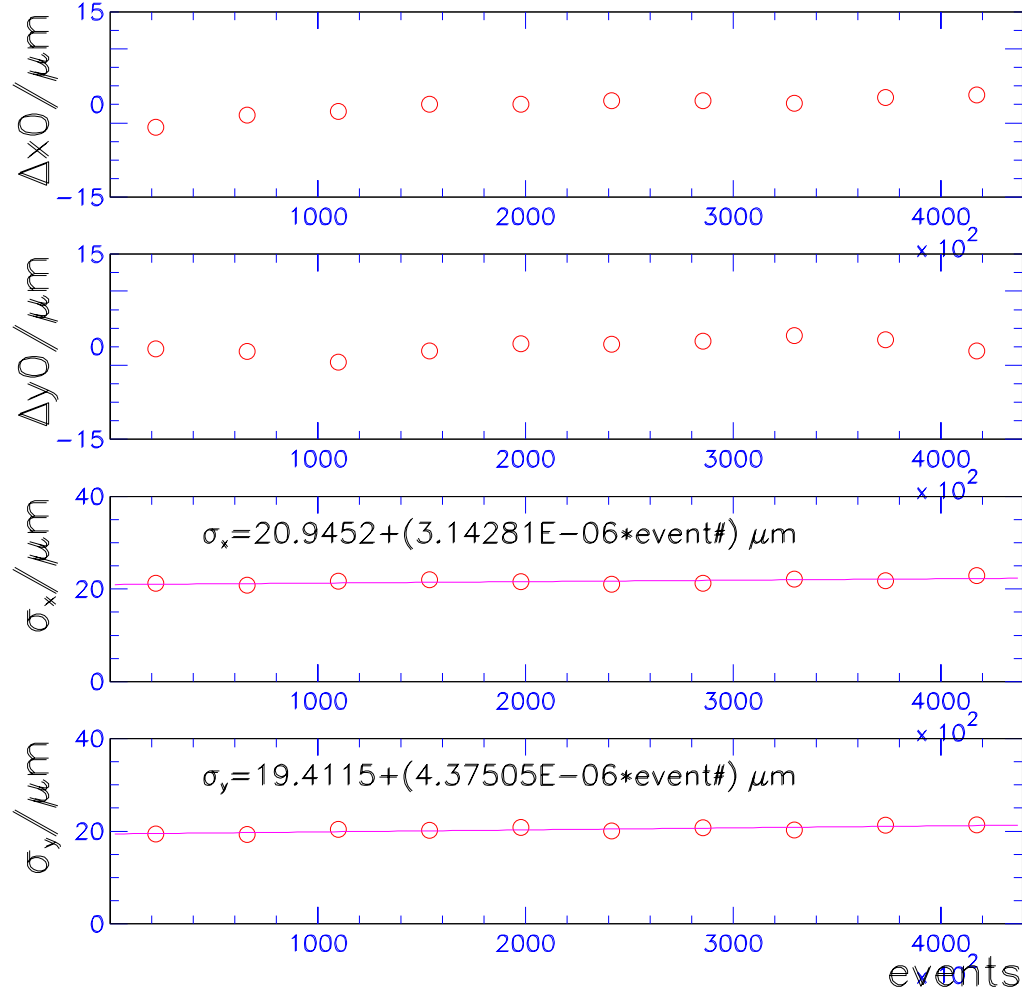


Figure 12: The upper two plots show the deviation in μm from the average beamposition as a function of time (event number) for the x and y projection respectively. The lower two plots show the width of the beam in μm as a function of time. Only vertices with $|z - z_0| < 10.\text{cm}$ have been used to estimate the width.

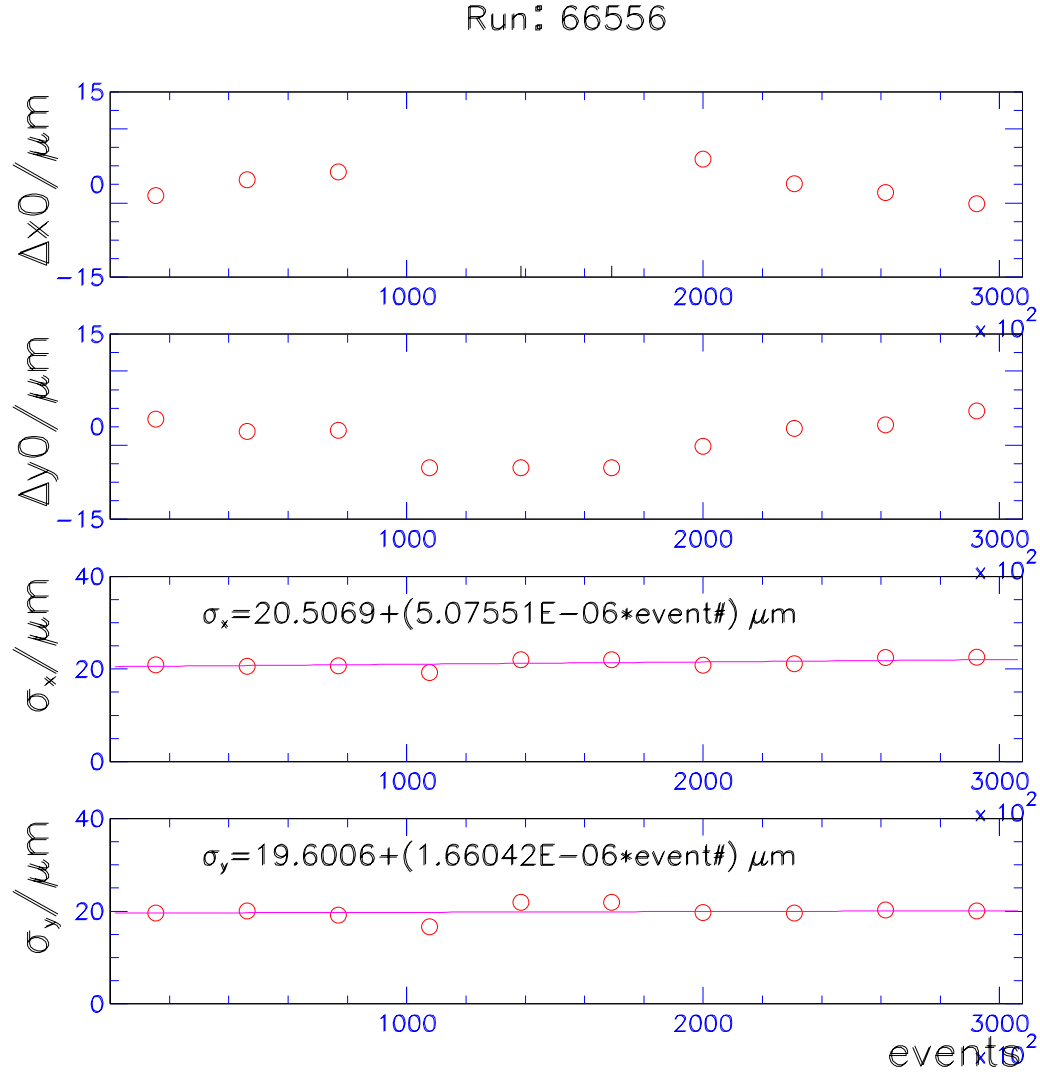


Figure 13: The upper two plots show the deviation in μm from the average beam position as a function of time (event number) for the x and y projection respectively. The lower two plots show the width of the beam in μm as a function of time. Only vertices with $|z - z_0| < 10.\text{cm}$ have been used to estimate the width.

Run: 68958

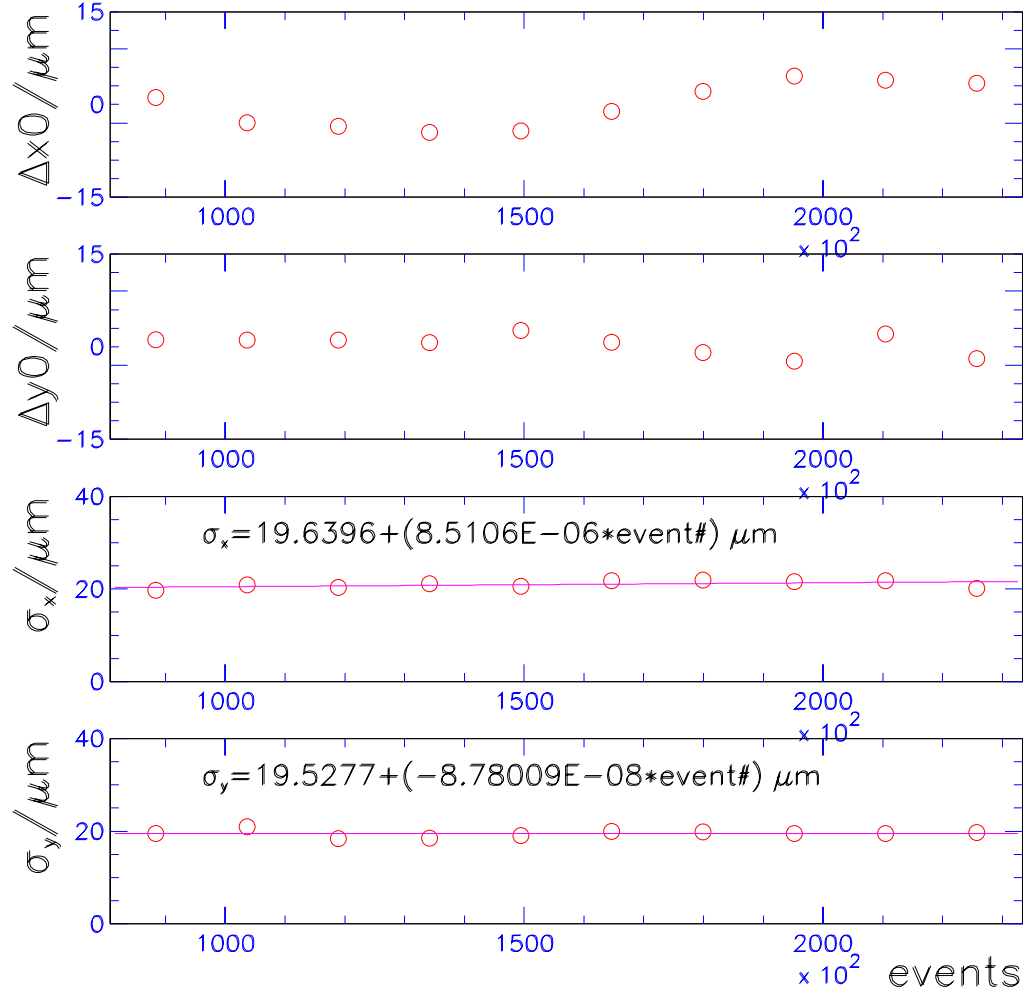


Figure 14: The upper two plots show the deviation in μm from the average beamposition as a function of time (event number) for the x and y projection respectively. The lower two plots show the width of the beam in μm as a function of time. Only vertices with $|z - z_0| < 10.\text{cm}$ have been used to estimate the width.

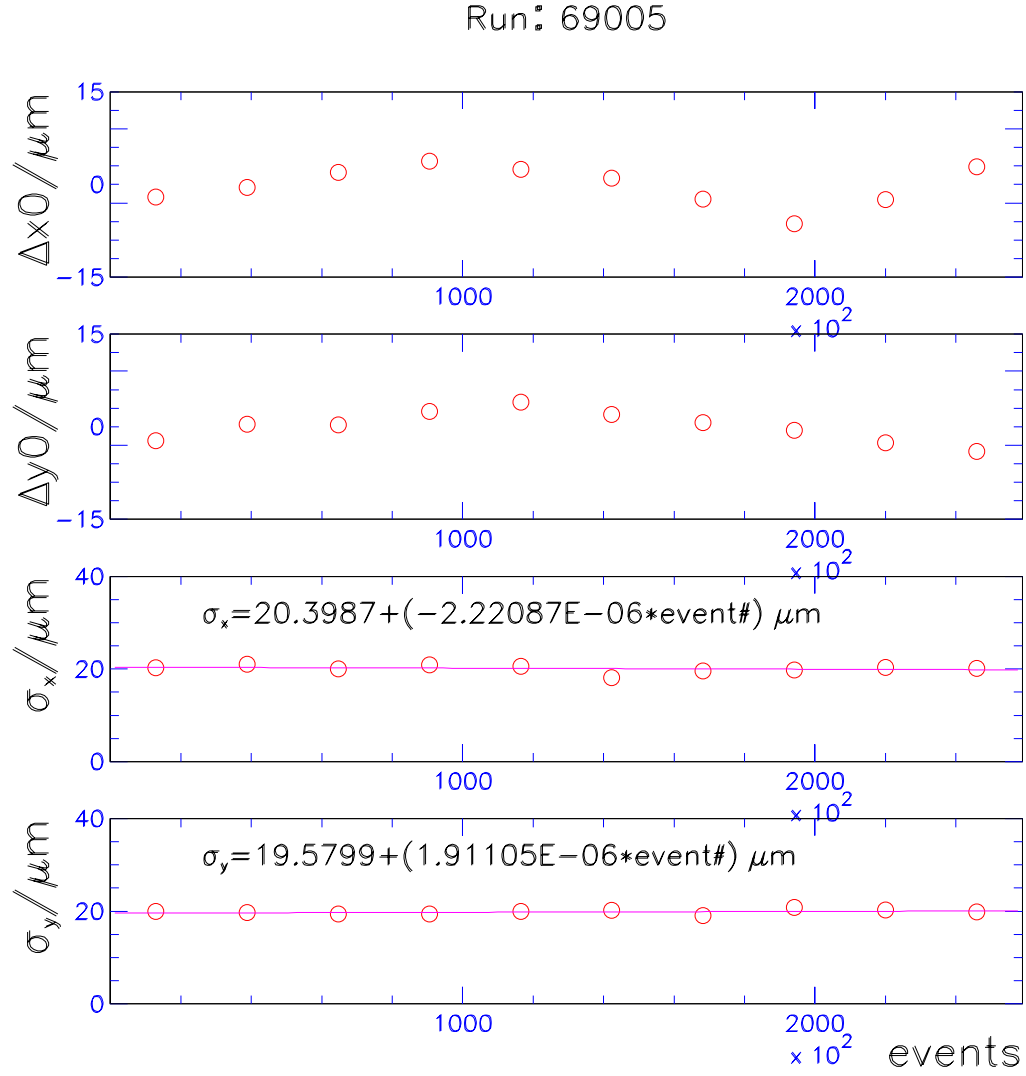


Figure 15: The upper two plots show the deviation in μm from the average beamposition as a function of time (event number) for the x and y projection respectively. The lower two plots show the width of the beam in μm as a function of time. Only vertices with $|z - z_0| < 10.\text{cm}$ have been used to estimate the width.

Run: 69354

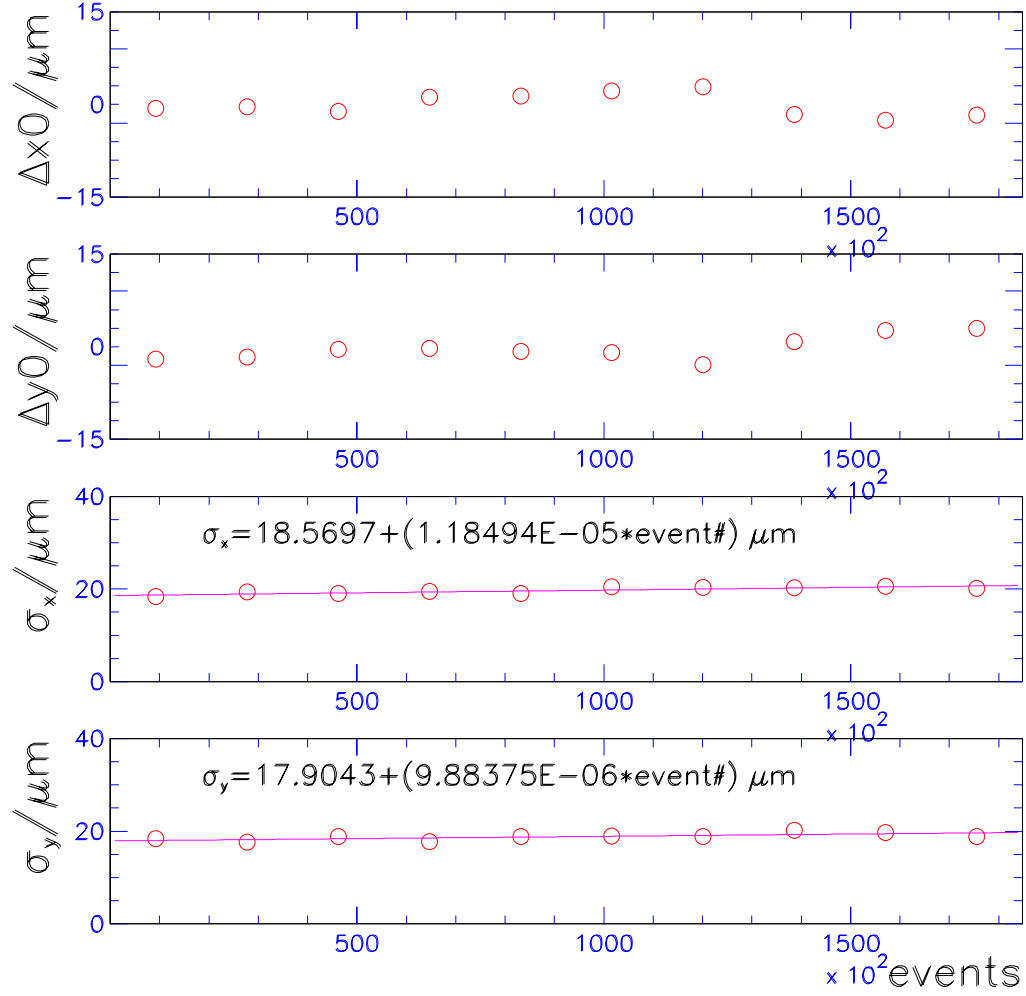


Figure 16: The upper two plots show the deviation in μm from the average beamposition as a function of time (event number) for the x and y projection respectively. The lower two plots show the width of the beam in μm as a function of time. Only vertices with $|z - z_0| < 10.\text{cm}$ have been used to estimate the width.

Run: 69392

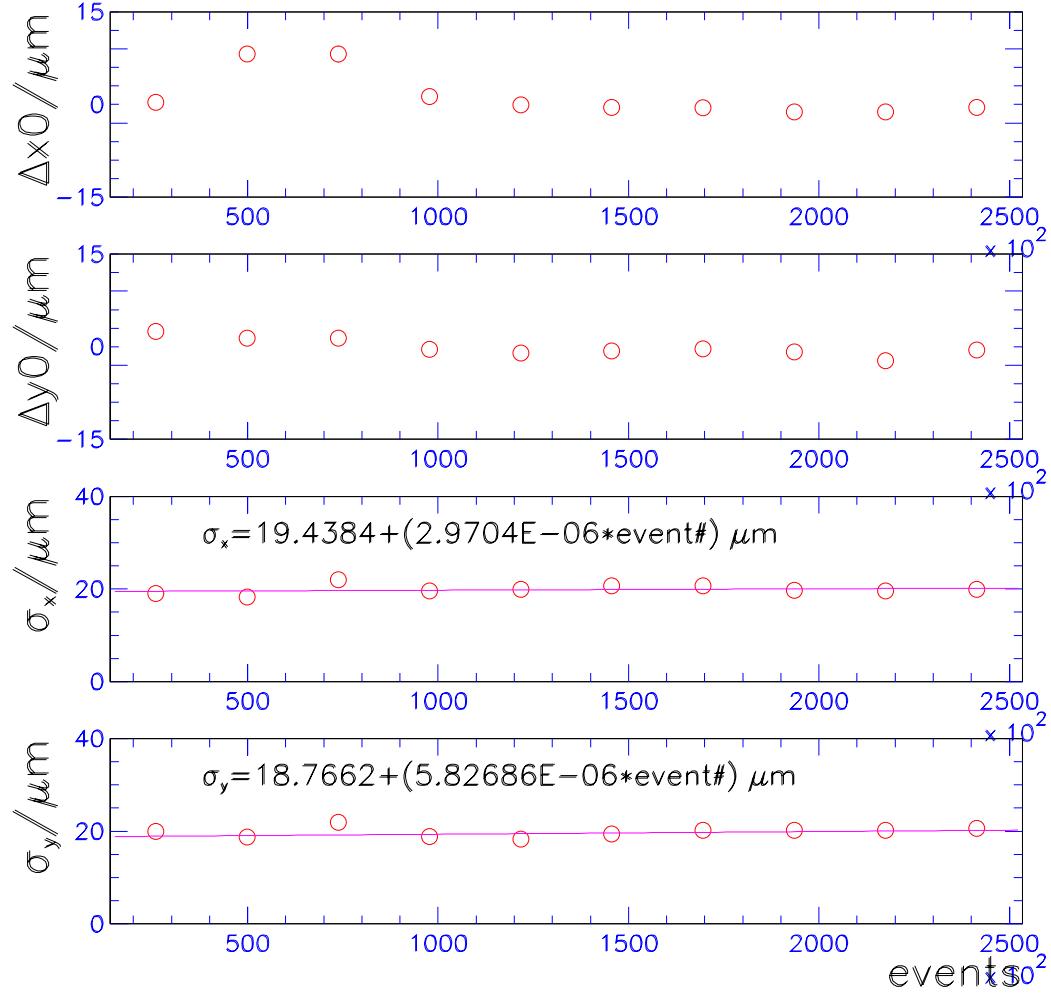


Figure 17: The upper two plots show the deviation in μm from the average beam position as a function of time (event number) for the x and y projection respectively. The lower two plots show the width of the beam in μm as a function of time. Only vertices with $|z - z_0| < 10.\text{cm}$ have been used to estimate the width.